A Study of the Influence of Thermomechanical Controlled Processing on the Microstructure of Bainite in High Strength Plate Steel

XIAOJUN LIANG and ANTHONY J. DEARDO

Steels with compositions that are hot rolled and cooled to exhibit high strength and good toughness often require a bainitic microstructure. This is especially true for plate steels for linepipe applications where strengths in excess of 690 MPa (100 ksi) are needed in thicknesses between approximately 6 and 30 mm. To ensure adequate strength and toughness, the steels should have adequate hardenability (C. E. >0.50 and Pcm >0.20), and are thermomechanically controlled processed, *i.e.*, controlled rolled, followed by interrupted direct quenching to below the Bs temperature of the pancaked austenite. Bainite formed in this way can be defined as a polyphase mixture comprised a matrix phase of bainitic ferrite plus a higher carbon second phase or micro-constituent which can be martensite, retained austenite, or cementite, depending on circumstances. This second feature is predominately martensite in IDQ steels. Unlike pearlite, where the ferrite and cementite form cooperatively at the same moving interface, the bainitic ferrite and MA form in sequence with falling temperature below the Bs temperature or with increasing isothermal holding time. Several studies have found that the mechanical properties may vary strongly for different types of bainite, *i.e.*, different forms of bainitic ferrite and/or MA. Thermomechanical controlled processing (TMCP) has been shown to be an important way to control the microstructure and mechanical properties in low carbon, high strength steel. This is especially true in the case of bainite formation, where the complexity of the austenite-bainite transformation makes its control through disciplined processing especially important. In this study, a low carbon, high manganese steel containing niobium was investigated to better understand the effects of austenite conditioning and cooling rates on the bainitic phase transformation, *i.e.,* the formation of bainitic ferrite plus MA. Specimens were compared after transformation from recrystallized, equiaxed austenite to deformed, pancaked austenite, which were followed by seven different cooling rates ranging between 0.5 K/s (0.5 °C/s) and 40 K/s (40 °C/s). The CCT curves showed that the transformation behaviors and temperatures varied with starting austenite microstructure and cooling rate, resulting in different final microstructures. The EBSD results and the thermodynamics and kinetics analyses show that in low carbon bainite, the nucleation rate is the key factor that affects the bainitic ferrite morphology, size, and orientation. However, the growth of bainite is also quite important since the bainitic ferrite laths apparently can coalesce or coarsen into larger units with slower cooling rates or longer isothermal holding time, causing a deterioration in toughness. This paper reviews the formation of bainite in this steel and describes and rationalizes the final microstructures observed, both in terms of not only formation but also for the expected influence on mechanical properties.

DOI: 10.1007/s11661-014-2444-5

I. INTRODUCTION

MICROALLOYED steels for construction, shipbuilding, or linepipe applications require not only high strength in steel plates, but also good toughness, weldability, and resistance to HIC and other hydrogen-related fractures.[1] The principal alloy and process design concepts have been known since before 1970 in ferrite–pearlite steels of lower strength levels near YS of 420 MPa.[2] These concepts include (1) reduction in the carbon contents and (2) combining the appropriate rolling parameters with proper microalloying to achieve a well-conditioned austenite. Achieving well-conditioned austenite involves rough rolling at high temperatures to reduce the austenite grain size and finish rolling at lower temperatures to change the austenite grain shape (controlled rolling), together with appropriate microalloying to raise the austenite recrystallization-stop

XIAOJUN LIANG, Postdoc Associate, is with the Department of Mechanical Engineering and Materials Science, Basic Metals Processing Research Institute, University of Pittsburgh, Pittsburgh, PA 15261. ANTHONY J. DE ARDO, Professor, is with the Department of Mechanical Engineering and Materials Science, Basic Metals Processing Research Institute, University of Pittsburgh, and also Distinguished Professor, with the Centre for Advanced Steel Research, University of Oulu, Oulu, Finland. Contact e-mail: deardo@pitt.edu
Manuscript submitted January 16, 2014.
Article published online July 17, 2014

temperature and increase the austenite near-planar interface area per unit volume (Sv); and (3) applying appropriate interrupted controlled cooling for the given CCT diagram to achieve the desired final microstructure.[2] However, in order to achieve a YS in excess of 690 MPa in heavier plates (6 to 25 mm), a matrix phase of bainitic ferrite is required, which forms together with a certain amount of unintended but unavoidable higher carbon second phase, micro-constituent or feature. This higher carbon second feature, which can be martensite, retained austenite, or cementite, depending on circumstances, is mainly martensite in low carbon, IDQ steels. This second feature will be referred to as ''MA'' in the remainder of the paper.

In this current paper, recent studies of high strength bainite in a 0.06 pctC steel will be presented. However, as indicated above, the term bainite is used to describe a wide range of specific and complex microstructures comprised of mixtures of the bainitic ferrite matrix phase and a high carbon second micro-constituent. Bainitic ferrite plus MA is often referred to as carbide-free bainite, since the excess carbon is tied up as high carbon martensite islands rather than as Fe_3C.[3] Unlike pearlite, where the ferrite and cementite form cooperatively, *i.e.*, at the same temperature, and at the same advancing transformation front, the bainitic ferrite plus MA in bainite forms separately at different temperatures or isothermal holding time.[4] Therefore, the microstructure represented by the generic term bainite can have many possible morphologies, where the various mixtures of bainitic ferrite and MA make it difficult to either describe or identify the structure in general, and can also lead to dramatic changes in properties. One recent example was illustrated by Zhu *et al.*,[5] in a very low carbon steel, *i.e.*, one with very little MA, where higher cooling rates from recrystallized austenite resulted in finer bainitic ferrite microstructures and higher tensile properties. A further complication arises because of the different thermal paths used in recent research studies: continuous cooling, isothermal, and IDQ. Even the same starting austenite might be expected to exhibit different bainite morphologies with the different thermal paths. This point has been clearly shown in a recent investigation by Huang *et al.*,[6] where the influence of the deformation of austenite in a very low carbon Mn-Nb-B steel followed by continuous cooling to room temperature at different cooling rates was observed to both accelerate the bainitic ferrite reaction and alter its microstructure.

Various attempts have been made to define or classify bainite in steels.[7–13] For example, Bramfitt and Speer[10] have attempted to classify continuously cooled bainite from its morphological perspective. Other attempts to describe or classify bainite in many types of steels have relied on the morphology, including location or the distribution of the second phases such as MA.[9] One goal of this current study is to help clarify the confusion concerning the description of bainite in low carbon steels.

Of course, any discussion of bainite formation, especially in low carbon steels, should include thermodynamics and kinetics. Over the past two decades, bainite formation has come to be understood as a diffusion-assisted, shear-type (displacive) transformation. It can be considered that the bainitic ferrite will form by a displacive type transformation, but the excess carbon will partition by diffusion to highly concentrated islands of austenite in the bainitic ferrite structure either within the ferrite grains or between the grains. In addition, a second form of MA is caused by the incomplete transformation of the austenite to bainite, and this untransformed austenite can also end up as MA, although of a lower carbon content. It therefore appears that there can be two sources of MA in DQ steels, that coming from carbon partitioning during the bainitic ferrite formation and that coming from the untransformed austenite. Due to the enrichment factor, one might expect the former to be of higher carbon content than that of the latter. These islands would then transform to high carbon martensite during subsequent cooling. Bainite transformation kinetics have been thoroughly studied, modeled, and discussed in high carbon, high silicon steels.[14–19] The kinetics of bainite formation start with the nucleation of the bainitic ferrite. It is now accepted that this ferrite forms by a displacive (shear-controlled) rather than a reconstructive (diffusion-controlled) transformation. Thus, the scale of the bainitic microstructure is known to be directly proportional to the driving force for the transformation.[18] Various kinetic models have been developed based on nucleation and growth.[15–17]

Bainite formation is also regarded as an autocatalytic reaction,[14–19] where the dislocations generated in austenite by one set of bainitic plates can help nucleate a second and later forming set of bainitic plates, in a fashion similar to that proposed by Bokros and Parker for the ''Burst Phenomenon'' in martensite.[20] It is believed that the autocatalytic nucleation can help explain the kinetics of bainite formation in high silicon, high carbon steels.[14–19] Whether this effect also pertains to low carbon, low silicon steels is unclear. However, the extent of the bainite reaction in steels seems limited by carbon partitioning during or after the transformation. Thus, in a high carbon steel, the bainite transformation usually needs sufficient time for carbon diffusion and then the growth of bainitic ferrite continues. In low carbon, high strength steel, the current research results showed that the bainitic transformation is very different from isothermal bainitic transformation in high carbon steel.[4] The bainitic microstructure should be simply considered as the mixture of bainitic ferrite and the second phase, normally MA in the low carbon bainitic steel. In this bainite, Fe_3C or other carbides are very difficult to form, either because of high activation energy of nucleation or due to the time needed to move the carbon; therefore, MA is the predominant second phase in bainite in most low carbon steels given reasonable plate rolling and cooling scenarios, especially IDQ. This MA is found either inside the bainitic ferrite grains or on the boundaries between them. It has been found that the formation of MA in the low carbon, high strength steel is strongly related to the carbon partitioning that accompanies the formation of the bainitic ferrite.[4] Experimental results have shown that MA is one of the

significant factors in the bainite microstructure in controlling the toughness of high strength steels, with low toughness associated with larger amounts and sizes of MA. Nevertheless, the bainitic ferrite itself is also a very critical factor for the overall mechanical properties of the steel.[5,6]

The morphology, size, or orientation of bainitic ferrite is usually determined by the packet size of the bainite, which has been shown to strongly affect cleavage cracking or FATT.[21,22] At the same time, there is very strong evidence that the MA distribution near the centerline can exaggerate hydrogen-related cracking or HIC.[23,24] The formation of MA has been discussed elsewhere.[4] The influence of TMCP on both the bainitic ferrite packet size, morphology, or orientation, and the accompanying MA appears to be important but the precise relationship is still not entirely clear in low carbon steels. Furthermore, the influence on kinetics and morphology of bainite by the plastic deformation of austenite, either from the hot rolling itself or by the formation of early bainitic packets or grains, is also not fully understood.[14] In this paper, a low carbon, high manganese bainitic steel was investigated to better understand some of the complexities described above. Observations of kinetics and microstructural details obtained, using EBSD and OIM techniques, were intended to gain some new insights into the bainite reaction in this class of steel. It is hoped that this new understanding will enable bainitic microstructures with improved mechanical properties to be obtained in low carbon, high strength steels by combining improved alloy design and TMCP.

II. EXPERIMENTAL PROCEDURE

The steel composition used in this study is shown in Table I. Ingots were laboratory melted in a vacuum induction furnace. Compression samples were machined from the ingots to study both the response of the austenite to the TMCP simulations and the resulting microstructures. Thermemcmastor-Z and MTS simulation systems were used in this program.

To simulate a typical plate rolling schedule where rough rolling for austenite grain refinement is first applied followed by finishing rolling for pancaking, two deformation stages in the simulators were used to first control the austenite grain size, and then second to increase the effective near-planar crystalline defect (grain boundary) area per unit volume or Sv. The critical temperatures for hot rolling are T_{95} and T_5.[25] Rolling above T_{95} results in complete recrystallization of the austenite, usually accompanied by grain refinement. Rolling below T_5 leads to pancaked austenite which is a desirable microstructure prior to final cooling. Rolling between T_{95} and T_5 can lead to mixed grain sizes and poor final microstructures and properties.[25] Therefore, the later region was avoided for hot rolling. The critical temperatures T_{95}, 1323 K (1050 °C), and T_5, 1198 K (925 °C), were determined in a separate experiment for the steel used in these experiments.[4]

In the experiment, one group of specimens was deformed with 5 consecutive 10 pct reductions at 1323 K (1050 °C) to simulate the roughing passes, and a second group received an additional 5 consecutive 10 pct reductions at 1123 K (850 °C) to simulate the finishing passes. Specimens were quenched into ice brine following the hot deformation from both 1323 K (1050 °C) and 1123 K (850 °C) to observe the prior austenite grain boundaries.

For each austenite condition, seven different cooling rates were compared for the bainite formation. During the tests, the dilatometric curves were recorded to create a CCT diagram. The purpose of this work was to obtain a better understanding of (1) bainite transformation from recrystallized or deformed austenite; (2) bainite formation under different cooling rates; and (3) the nucleation of bainitic ferrite and its subsequent coarsening.

After the plate rolling simulation using frictionless or homogeneous compression and controlled cooling tests, the specimens were sectioned, polished, and etched in a 2 pct nital solution. The microstructures near the centerline were observed by optical microscopy and with a Philips field-emission-gun SEM (XL-30). EBSD results were collected and analyzed by the TSL EBSD equipment attached to the Philips SEM XL-30 and orientation imaging microscopy.

III. RESULTS AND DISCUSSION

The microstructures of the prior austenite grains after the five roughing passes and after the roughing plus five finishing passes are shown in Figures 1(a) and (b), respectively. The average equivalent diameter of the pancaked austenite is about 43.9 ± 10.1 μm, which is very close to the average austenite grain size in Figure 1(a), and about 46.0 ± 13.6 μm after deformation at 1323 K (1050 °C); that is, the non-recrystallization region rolling only leads to pancaked austenite grain shapes and an increase in the effective grain boundary area (the surface area of austenite grain boundaries per unit volume Sv), but the average grain volume was essentially not changed.

A. *Bainite Transformation from Recrystallized Austenite*

In this current experiment, bainite formation was investigated inside the prior austenite grains after being

Table I. Steel Composition, Weight Percent

C	Mn	P	S	Si	Cu	Ni	Cr	Mo	Ti	Al	N	Nb	B
0.06	1.89	0.009	0.0016	0.29	0.24	0.24	0.49	0.24	0.01	0.023	0.0046	0.039	0.0005

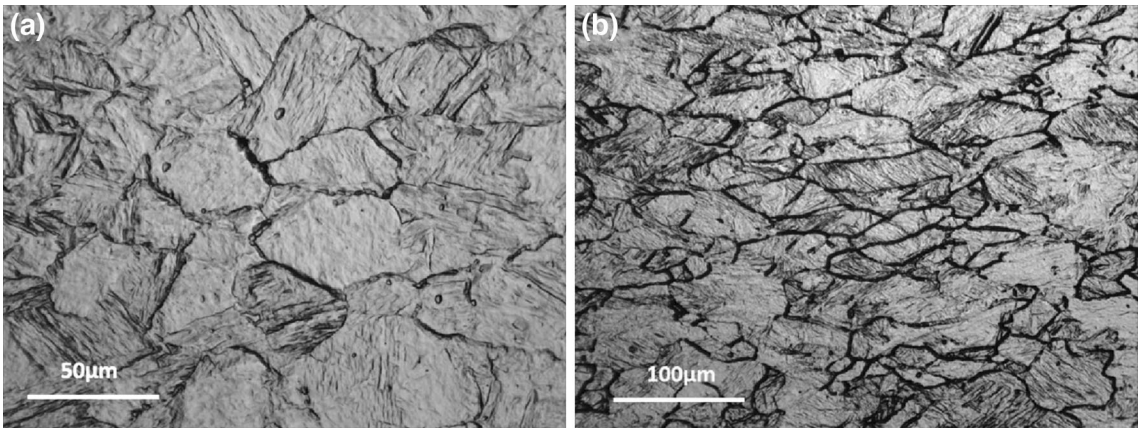

Fig. 1—(*a*) Austenite grain boundaries after five 10 pct consecutive deformation at 1323 K (1050 °C); (*b*) pancaked austenite grain boundaries after additional five 10 pct consecutive deformation at 1123 K (850 °C).

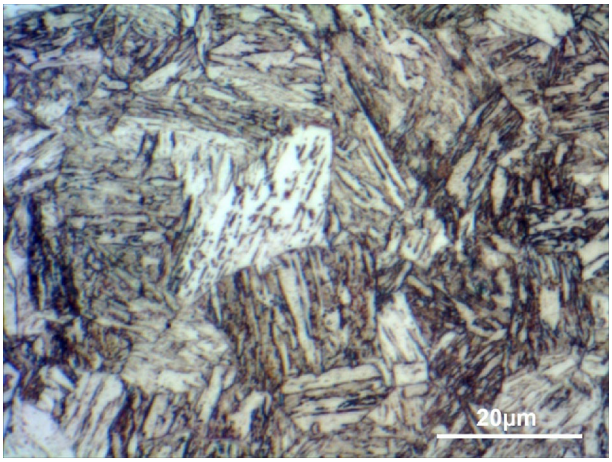

Fig. 2—Optical microstructures of the initial stage of bainite formation. The sample was cooled to 773 K (500 °C) with the cooling rate of 25 K/s (25 °C/s), and the sample was water quenched to room temperature. Nital etched.

nucleated on the austenite grain boundaries. Figure 2 shows the microstructures water quenched from 773 K (500 °C) after the sample was cooled at 25 K/s (25 °C/s) to 773 K (500 °C), and water quenched with no holding time. This condition was used to observe the initial stages of the bainitic ferrite formation (white appearance). It can be seen that most of the area is martensite transformed from austenite during water quenching. But it can be also easily observed that some bainitic laths have been formed at the initial stage at or near 773 K (500 °C).

More results are shown in Figure 3 for the case of recrystallized austenite, where very different bainitic ferrite morphologies can be observed when the cooling rates from 773 K (500 °C) to RT varied from 0.5 K/s (0.5 °C/s) to 10 K/s (10 °C/s). The microstructure is observed to be mainly lath martensite when the cooling rate is faster than 20 K/s (20 °C/s). In this specific steel, it is apparent that there is no new polygonal ferrite formation along the prior austenite boundaries, or at other preferential areas such as inclusions and defects, even when the cooling rate is as low as 0.5 K/s (0.5 °C/s).

The two features of prime importance in describing bainitic ferrite are packet size and crystallographic orientation. These features are also important when discussing mechanical properties of bainitic steels. Bainitic ferrite transformation is similar to the martensite transformation since both exhibit displacive type transformation characteristics. However, one of the main differences between martensite and bainite is the carbon partitioning. Since the Bs temperature is normally about 150 K (150 °C) to 200 K (200 °C) higher than that of Ms temperature, carbon has enough mobility to partition during the bainite transformation. However, little movement of the substitutional elements can be expected, which has been shown by Caballero's atom probe results.[26] In Figures 3(a) through (f), the microstructures are typical of the bainite microstructures observed. Figures 3(a) and (b) exhibit the bainitic ferrite and a high volume fraction of MA due to more time for carbon partitioning available at the slow cooling rates. In the slowly cooled steel, the bainitic ferrite is more likely to be rather coarse in scale. Very few ferrite grain boundaries devoid of MA can be observed in the slow cooled samples. However, when the cooling rates increased, the bainitic ferrite plates became smaller. The bainite microstructure appears to be very close in morphology to the martensite microstructure when the cooling rate is rapid.

When describing bainite, traditional descriptions such as upper and lower bainite have been used.[8,27] This approach is suitable when the steel contains relatively high carbon contents, and the relatively large amount of Fe_3C aids in the classification. However, the situation is very different in low carbon steels, where the so-called carbide-free bainite is observed. The results of this current study agree with earlier work of Bhadeshia[7–13] that suggested that traditional lower bainite, by definition, probably does not exist in low carbon steels. However, the term lower bainite has been used in several recent publications. This confusion may originate in the complex morphology of low carbon bainite, which cannot be easily classified as upper bainite or lower

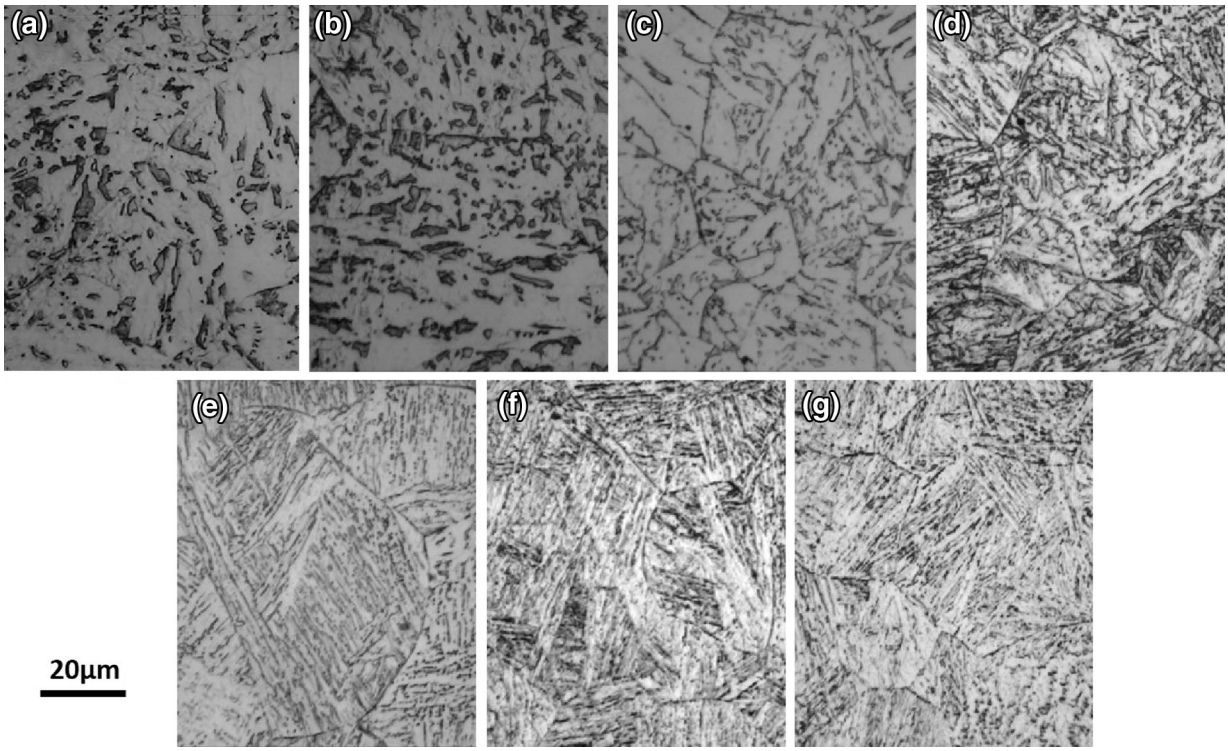

Fig. 3—Optical microstructures of bainite transformation in samples from undeformed austenite with the cooling rates of: (*a*) S1: 0.5 K/s (0.5 °C/s), (*b*) S2: 1 K/s (1 °C/s), (*c*) S3: 2 K/s (2 °C/s), (*d*) S4: 5 K/s (5 °C/s), (*e*) S5: 10 K/s (10 °C/s), (*f*) S6: 20 K/s (20 °C/s), and (*g*) S7: 40 K/s (40 °C/s).

bainite. Lower bainite is defined by having intragranular precipitation of Fe_3C. Perhaps when the bainitic ferrite in low carbon steels has MA inside the bainitic grains, this might cause it to be mis-identified as lower bainite. In a similar fashion, so-called carbide-free bainite might be a somewhat mis-leading description since the excess carbon partitioned from the ferrite and normally found in Fe_3C in bainite probably has been replaced by high carbon MA.

IV. AUTOCATALYSIS

At the higher cooling rates, the bainite has many fine bainitic ferrite laths instead of a few large plates. This means that there is a larger driving force for bainitic ferrite nucleation at higher cooling rates. This results in finer bainitic ferrite grains. Since the formation of bainitic ferrite appears to have an autocatalytic component, this has been used to describe the nucleation rate.[17]

$$\frac{df}{dt} = (1-f)(1+\lambda f)v\frac{Z\delta}{D^{\gamma}}\alpha_B(T_h - T)\exp\left(-\frac{Q^*}{\mathrm{RT}}\right) \quad [1]$$

where f is the fraction of bainite as a function of time t; λ is a autocatalytic factor; v is an attempt frequency; Z is a geometrical factor; δ is a constant; D^{γ} is the austenite grain size; and α_B is the kinetic parameter describing the rate of bainite formation. T_h is assumed the start of the bainite transformation temperature, or the Bs. The autocatalytic factor λ determines the relative contribution of autocatalysis to the overall kinetics. The temperature dependence of the kinetics is mainly governed by $(T_h - T)$ and the T in the exponent.

The autocatalysis factor λ is described to be smaller when the carbon content is higher, as shown in Eq. [2][15]:

$$\lambda = k_1(1 - k_2 x) \quad [2]$$

k_1 and k_2 are the constants and x is the carbon concentration in the steel. This may be because carbon is enriched mainly in austenite near the tip of bainitic ferrite plates, where most dislocations in austenite resulting from the transformation would be expected. Therefore, these austenite regions are chemically more stable and mechanically stronger and would therefore resist the lengthening of the plates and the overall progress of the transformation.

In the low carbon steel, it was found that the bainitic transformation was completed in several seconds to tens of seconds during continuous cooling. The isothermal treatment results also show that bainite formation can be completed in approximately 1 minute.[4] This shows, therefore, that the reaction can be completed very rapidly in low carbon steel due to its high autocatalysis factor, the large temperature difference or supercooling and the small activation energy barrier for bainite formation at high cooling rates.

Figure 4 shows the CCT curves of the steel with and without deformation. As indicated by symbols in the figure, the bainite start temperature is higher both from deformed austenite and with slower cooling rates:

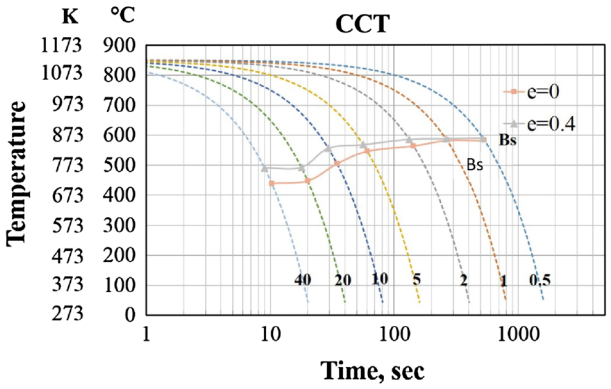

Fig. 4—CCT diagrams without (e = 0) or with austenite (e = 0.4) deformation.

0.5 K/s (0.5 °C/s) to 2 K/s (2 °C/s). And the Bs temperature gradually decreases when faster cooling rates were used. The cooling rate effect, *i.e.*, the variation of Bs at slow versus fast cooling, is about 100 K (100 °C) for the deformed austenite and about 150 K (150 °C) for the undeformed austenite. The lower temperature reaction has the higher driving force as analyzed by thermodynamics. Thus, it can be assumed that the bainite displacive transformation is strongly dependent on the driving force, that is, the difference of free energy between the newly formed bainitic ferrite and the original austenite. At a slow cooling rate, the relative shear movements of iron atoms in the lattice can be assumed to be very small due to a small driving force. This correlates very well with the observation that only very low angle boundaries can be seen by EBSD in the slowly cooled specimens. In some cases, even these relative movements appear to be negligible in some grains. Examples are shown in Figures 2(a) and (b). Consequently, assuming solute carbon in iron, then no carbon diffusion should be expected during transformation in the displacive model, and the remaining fcc austenite would still continue transforming into a bcc-based ferrite microstructure, as a massive type transformation, *i.e.,* at constant composition. However, it would not be bainite according by definition, since there is no MA formed in this scenario. Interestingly, the predicted large grained ferritic microstructure is observed in some other alloys.[28] Furthermore, the transformation orientation would be expected to vary with cooling rate and driving force,[28] because the amount of driving force should affect the distance of the lattice displacements. If one considers the diffusion of carbon in a very low carbon steel, during displacive movement, defects are very easily introduced; thus, carbon can partition preferentially to these defect areas such as grain boundaries and dislocations. Carbon partitioning is a time- and temperature-sensitive process. In the extreme case at very long holding times or slow cooling rates, it can be observed that the bainitic ferrite reversely transforms back to austenite due to carbon partitioning during isothermal holding.[4]

Due to the limitation of optical microscopy or scanning electronic microscopy, only the morphological details can be observed, which are insufficient to show the real evidence of the formation of bainitic ferrite, or its internal structure. However, EBSD is a technique that can make up for the above-mentioned limitation. With the aid of Kikuchi patterns, the orientation information of each grain can be recorded, and thus some information on related grain boundaries and orientations can be easily obtained. The scanning step size of EBSD analysis can be set as small as 0.1 to 0.2 μm, depending on the morphologies and scale of the microstructures.

Figures 5(a) and (b) are reconstructed images by EBSD techniques for the samples with the cooling rate of 2 K/s (2 °C/s) and 10 K/s (10 °C/s). The microstructure is superimposed with different colors which are used to distinguish the different orientations in inverse pole figures. Only high-angle grain boundaries (>15 deg) are reconstructed in the figures as black lines. Apparently, there are far fewer high-angle grain boundaries in Figure 5(a) when compared to the sample with the cooling rate of 10 K/s (10 °C/s), as shown in Figure 5(b). In Figure 5(a), the prior austenite grain boundaries can be clearly observed. Thus, it can be easily seen that very few high-angle grain boundaries exist inside some austenite grains in the bottom of Figure 5(a). This means that during the bainite transformation, in those austenite grains, most bainite laths have similar orientations. However, in Figure 5(b), due to the faster cooling rate, the relative lattice movements should be higher; thus, more bainitic ferrite laths have been identified and also the clearly defined high-angle grain boundaries between the laths have been observed. The width of bainitic ferrite appears to be related to the transformation temperature. This may be because of two reasons: (1) higher driving forces can cause strong shear movement with smaller distances between the active shear planes in the austenite leading to more narrow laths. The strong shear movement might also be expected to result in imperfect atomic movements and (2) during continuous cooling, faster cooling rates provide higher driving force, which can create more nucleation sites and increase nucleation rates according to nucleation kinetics. Furthermore, some new austenite/bainitic ferrite boundaries can also become additional nucleation sites for the new bainitic ferrite formation, in addition to the prior austenite grain boundaries. Hence, different bainitic ferrite laths of different sizes and orientations may be formed at different temperatures. Also, less coarsening and coalescence would be expected at higher cooling rates. Finally, the MA found in the bainitic ferrite appeared to be the result of the incomplete transformation of austenite and not the repartitioning of carbon from the bainitic ferrite forming new austenite. The amount and size of the MA appeared to fall as the cooling rate was increased from 0.5 K/s (0.5 °C/s) to 20 K/s (20 °C/s) as shown in Figures 2(a) through (f).

A. *Bainite Transformation from Deformed Austenite*

The bainite coming from the austenite with deformation was also studied to compare the effect of the

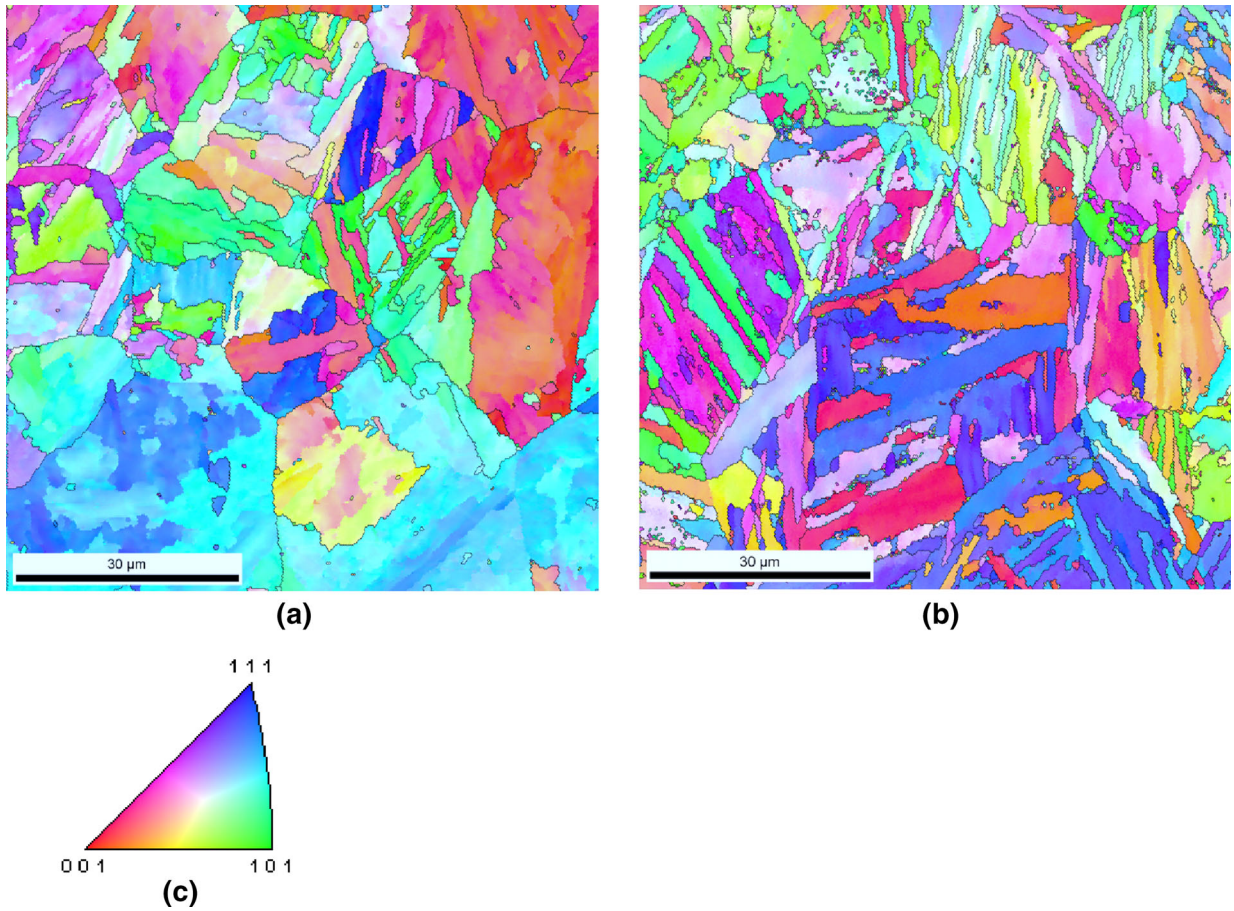

Fig. 5—The EBSD images with inverse pole figure and high angle grain boundaries. (*a*) S3: 2 K/s (2 °C/s), (*b*) S5: 10 K/s (10 °C/s), and (*c*) inverse pole figure key.

pancaked (deformed) and equiaxed (recrystallized) austenite grain structure on the bainite formation. The pancaked austenite can have more nucleation sites due to the increased grain boundary surface areas per unit volume, which is supposed to accelerate the bainite formation. Also, after controlled rolling, the free energy and defect structure of the deformed austenite can be expected to be higher due to the retained strain. This would also increase the amount of supercooling to the Bs temperature and increase the driving force for the transformation. Bhadeshia[14] has reviewed some issues concerning stabilization in the bainite transformation. In his review, Bhadeshia[6,19,29,30] compared literature data showing both stabilization and acceleration of the bainite reaction caused by the deformation of austenite during the isothermal transformation of high carbon austenite. Some publications show that the deformation acted to stabilize the austenite, and thereby the bainite transformation temperature is lower.[29,30] But the Huang *et al.*[6] research work showed the completely different trend for the bainite transformation. The Huang *et al.* results indicated that the bainite start transformation temperatures were raised in ultra-low carbon steels after deformation, which are consistent with the observations made in the current study in low carbon steel. Comparing these steels by carbon content, the stabilization found in high carbon steel is probably caused by the high carbon content in the steels studied, as discussed above for the case of bainite coming from undeformed austenite. The dislocation structure resulting from the formation of the bainite of early formation will deform the remaining austenite, *i.e.*, the autocatalytic effect. These dislocations will attract solute carbon which will locally thermodynamically stabilize and mechanically strengthen the austenite, resisting further transformation and causing the Bs temperature to be lowered. This mechanical strengthening may be similar to dynamic strain aging of the austenite. The appearance of MA, inter-lath carbide, and retained austenite in bainite in higher carbon steels substantiates the carbon partitioning effect.[31] Therefore, the high carbon concentration can inhibit the continuous transformation from austenite to bainitic ferrite.

However, in low carbon steel, the growth of bainitic ferrite is known to be very rapid, probably caused by the lower amount of carbon to be partitioned and the lower dislocation density resulting from the autocatalytic effect in the remaining austenite. The stabilization effect in this case would be weaker, the transformation would not be strongly slowed or inhibited, and the faster kinetics would expected. And the two factors short carbon partitioning time and low carbon content, result

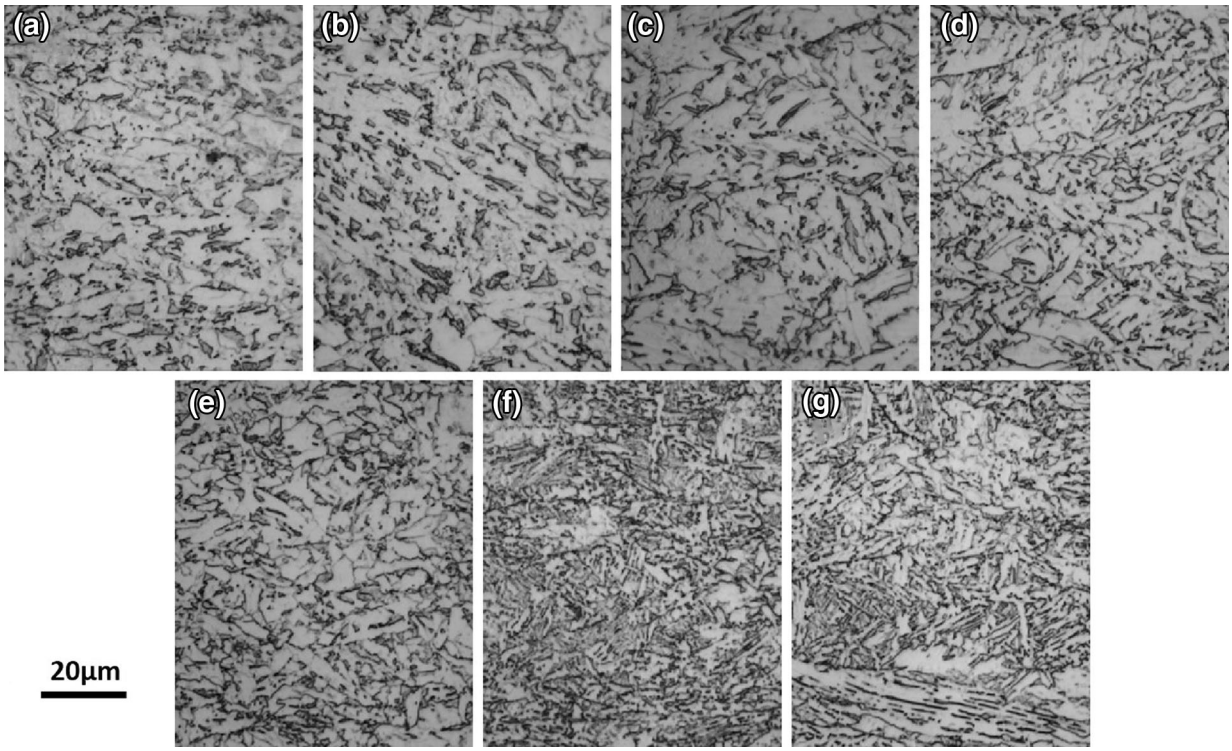

Fig. 6—Optical microstructures of bainite transformation in samples with deformed austenite (40 % reduction at 1123 K (850 °C)) with the cooling rates of: (*a*) D1: 0.5 K/s (0.5 °C/s), (*b*) D2: 1 K/s (1 °C/s), (*c*) D3: 2 K/s (2 °C/s), (*d*) D4: 5 K/s (5 °C/s), (*e*) D5: 10 K/s (10 °C/s), (*f*) D6: 20 K/s (20 °C/s), and (*g*) D7: 40 K/s (40 °C/s).

in few carbon-rich regions in the remaining austenite. The carbon concentration is not high enough to prevent bainitic ferrite growth by the displacive mode.

Thus, a strong stabilization phenomenon cannot be observed in low carbon steel. On the other hand, the deformed austenite increases the grain boundary surface area per unit, and therefore, provides more nucleation sites for bainite formation. Furthermore, the deformed austenite usually has more stored energy. Supposing the free energy of original austenite is $G\gamma$, and after deformation the stored strain energy can be taken as ΔG_d. Then, the driving force for bainitic ferrite formation would be as shown in Eqs. [3] and [4]:

$$\Delta G_v = G_\alpha - G_\gamma, \text{ undeformed austenite,} \qquad [3]$$

$$\Delta G_v^d = G_\alpha + \Delta G_d - G_\gamma, \text{ deformed austenite,} \qquad [4]$$

Upon comparing the two Eqs., [3] and [4], it can be seen that the driving force for bainite formation is higher for the deformed austenite, which promotes higher nucleation rates of bainite formation. One might consider that the relatively large local dislocation density in the austenite coming from the deformation and the autocatalytic effect, together with the partitioned carbon, would retard the bainite reaction. However, perhaps the dislocations alone, without substantial carbon pinning, cannot materially slow down the bainite formation. Thus, the bainite formation temperature might be elevated. The measured bainite start transformation temperatures are plotted in Figure 4. The pancaked austenite not only increased the austenite grain boundary surface area per unit volume, but also increased the deformation bands and dislocations, hence the pancaked austenite has high stored energy as the driving force for transformation. In Figure 4, it is found that the bainite transformation temperatures can be raised about 50 K (50 °C) for the pancaked austenite. The nital-etched microstructures in the steel cooled with the seven cooling rates are shown in Figure 6. Due to the increased driving force from the strain energy, all the microstructures are some form of bainite according to the optical micrographs, even if the cooling rate was increased to 40 K/s (40 °C/s). Obviously, the deformed austenite has acted to reduce or eliminate the martensite found with the undeformed austenite.

On the other hand, the size of the bainitic ferrite grains coming from the deformed austenite is obviously much finer than those from undeformed austenite. This refinement is a result of the austenite grain boundary surface area increasing and the formed deformation bands or dislocations after the deformation in the non-recrystallization region. However, it is still considered that the bainitic ferrite has formed by the displacive reaction. Similarly, with the slow cooling rate, no clear bainitic ferrite grain boundaries can be observed, as shown in Figures 6(a) and (b). The SEM micrographs in Figure 7 further show the higher magnification of microstructures of samples D1, D2, and D7 in Figure 6, which are the microstructures of the samples

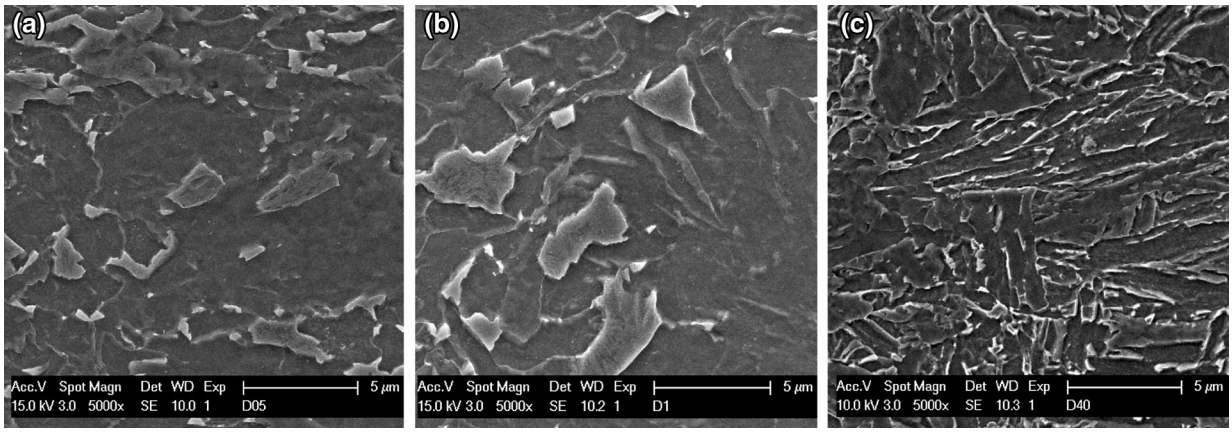

Fig. 7—SEM microstructure of samples (*a*) D1: 0.5 K/s (0.5 °C/s), (*b*) D2: 1 K/s (1 °C/s), and (*c*) D7: 40 K/s (40 °C/s).

with the cooling rate of 0.5 K/s (0.5 °C/s), 1 K/s (1 °C/s), and 40 K/s (40 °C/s), respectively. At the slow cooling rate, the size of the bainitic ferrite is large and some large MA constituents are distributed between the bainitic ferrite grains. When the cooling rate was increased to 40 K/s (40 °C/s), the microstructure was refined and the bainitic ferrite appeared to change character, from approximately equiaxed with slow cooling to being lath-like at faster cooling. A large portion of the MA also changed character with increased cooling rate. At the slower cooling rates, the MA also exhibited an equiaxed shape but with a bimodal size distribution, with one group smaller than approximately one micron and the second approximately 2 to 5 μ. However, at the higher cooling rate, the MA assumed a sheet-like morphology at the ferrite grain boundaries, perhaps reflecting the change in shape of the ferrite with cooling rate. Furthermore, the texture can be more random in the deformed samples since austenite may be divided into several parts by deformation bands or some sites with increased driving forces for starting a new transformation. This can be observed in the EBSD results.

Figures 8(a) and (b) are the reconstructed images of the EBSD results of the two samples D3 and D7 using orientation imaging through the inverse pole figure technique. The arrow in the figure indicates the rolling direction of the samples. Comparing to Figure 5, the size of the bainitic ferrite coming from deformed austenite is much smaller, *viz*. Figures 5 and 8. However, the outlines of a few prior austenite grain boundaries can still be observed. Two typical austenite grains are indicated with black solid lines. These two pancaked austenite grains are nearly parallel to the simulated rolling direction, as indicated by arrows. Although the texture of the specimens is more random with the deformed austenite, the orientations of bainite should be strongly related to the mother phase, the prior austenite texture. Some of the bainitic ferrite can be observed to be inherited from the same austenite grains and retained very similar orientations. These bainitic ferrite grains grow inside of the austenite and do not extend beyond the prior austenite grain boundary.

V. THE THERMODYNAMICS AND KINETICS OF THE FORMATION OF LOW CARBON BAINITE

As discussed in the earlier sections, the bainite start temperature, bainite unit size, orientation, and nucleation rate appear to be related to the difference in free energy between the parent austenite and bainitic ferrite. In this section, an attempt is made to discuss in more detail the thermodynamics and kinetics of the formation of bainite in low carbon steels. It is well known that during continuous cooling, the undercooled austenite can develop sufficient driving forces for various transformations at different undercooled temperatures, *i.e.*, polygonal ferrite, non-polygonal ferrite, acicular ferrite, bainitic ferrite, and martensite.

When austenite is cooled, it is also understood that there can be three types of transformations, depending on the driving force and transformation temperature: Diffusion-controlled or reconstructive transformation can occur at low supercooling (*e.g.*, polygonal ferrite), shear-type or displacive transformation at high supercooling (*e.g.*, martensite), and a mixed mode at intermediate supercoolings (*e.g.*, bainite). In the diffusion-controlled polygonal ferrite formation, the Ae3 temperature is a critical factor for the transformation. However, in the displacive controlled transformation, T_0 is used as the critical temperature for transformation. T_0 is defined as the temperature at which the two phases (austenite and bainitic ferrite) have the same free energy. Thus, we can use the T_0 hypothesis and definition to explain the driving force and nucleation rate for bainite formation.

For an undercooling ΔT ($\Delta T = T_0 - T$, where T is the undercooled temperature), if the difference in the specific heats of austenite and bainite can be ignored, then the volume free energy can be expressed as Eq. [5]:

$$\Delta G_v = \frac{L_v \Delta T}{T_0}, \qquad [5]$$

where Lv is the latent heat of phase transformation from austenite to bainite cooled with a non-equilibrium route.

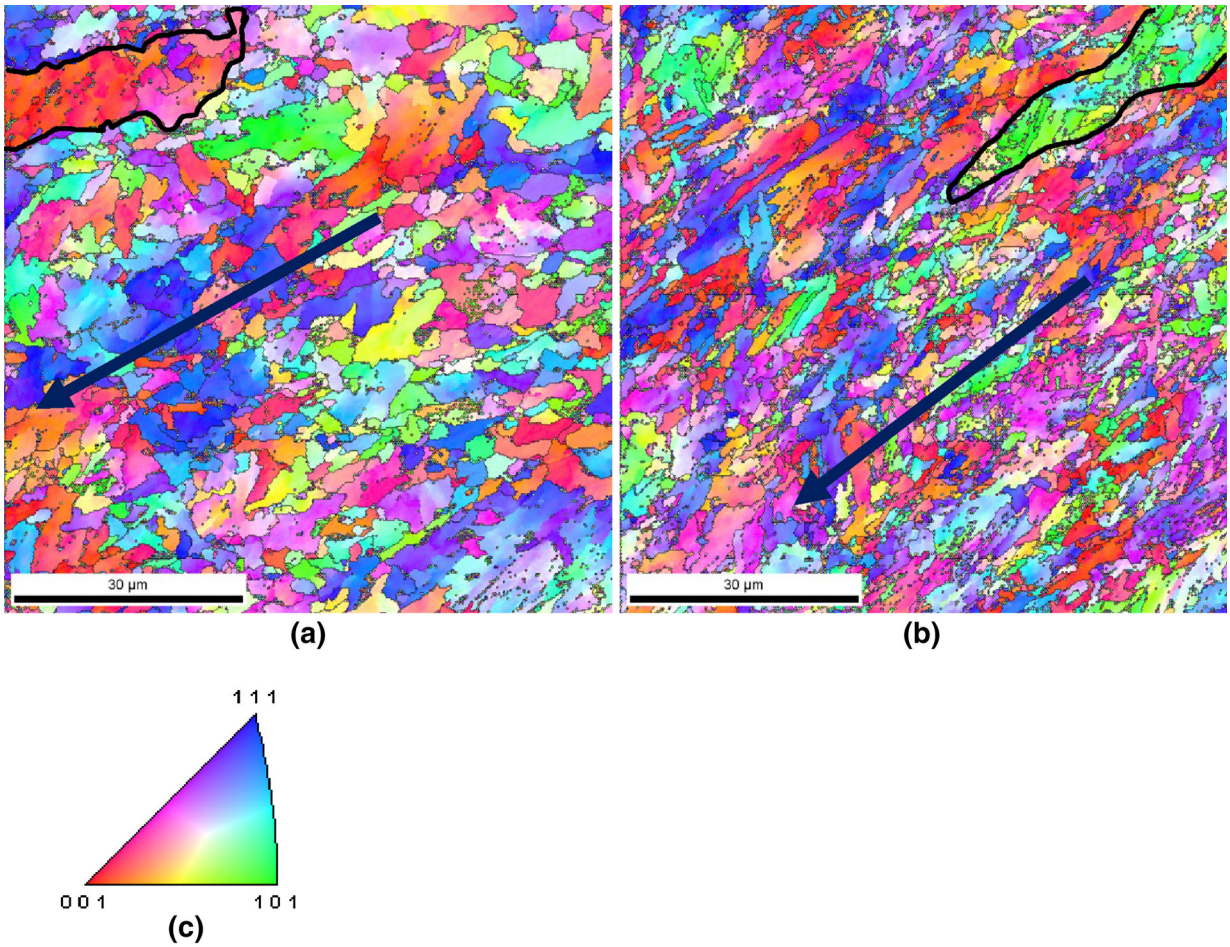

Fig. 8—The EBSD images with inverse pole figure and high angle grain boundaries. (*a*) D3: 2 K/s (2 °C/s), (*b*) D7: 40 K/s (40 °C/s), and (*c*) The standard triangle showing the color-coded directions used in (a) and (b).

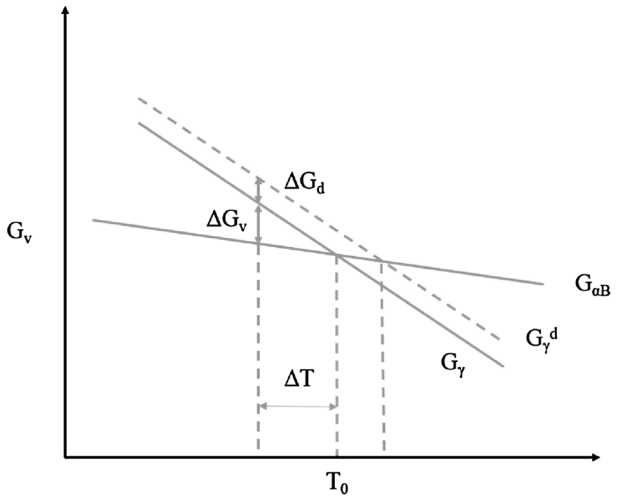

Fig. 9—Schematic diagram of free energy changes for austenite-bainite transformation.

If we assume bainite nucleation is a simple form of heterogeneous nucleation,[32] and neglect strain energy caused by lattice misfit considerations, then the activation energy barrier can be written as Eq. [6]:

$$\Delta G^* = \frac{16\pi E_{\alpha\gamma}^3}{3\Delta G_v^2} \cdot S(\theta) \qquad [6]$$

where $E_{\alpha\gamma}$ is the interfacial energy between ferrite and austenite and $S(\theta)$ is the shape factor.

Thus, according to the Eqs. [5] and [6], and as has been discussed many times in the past, a larger undercooling ΔT can cause a smaller ΔG^*. That means the larger undercooling can cause a high nucleation rate. Autocatalysis was used to explain nucleation in Eq. [1].[15] Thus, the low carbon steel has a higher autocatalytic factor. This is supposed to be the reason that bainite formation can be completed in a very short time in low carbon steel, even though there is a portion of the transformation that is diffusion controlled. That is, in low carbon steel, the formation of bainite is dependent more on nucleation than on bainitic growth.

With the combined consideration of bainite formation from austenite with and without deformation, it is concluded that the size of bainitic ferrite is very much related to the controlled cooling rates. A schematic diagram of Gibbs free energy is shown in Figure 9. The deformation increases the free energy of austenite, ΔG_d,

thus, the free energy change between deformed austenite and bainitic ferrite also increases.

$$\Delta G_v^d = \Delta G_v + \Delta G_d \quad [7]$$

According to the Eq. [8]:

$$\Delta G_d^* = \frac{16\pi E_{\alpha\gamma}^3}{3\Delta G_v^{d^2}} \cdot S(\theta), \quad [8]$$

a smaller activation energy barrier is necessary for higher nucleation rates. Hence, the higher nucleation rate causes the smaller size of bainitic ferrite or the more random bainitic ferrite orientations.

VI. CONCLUSIONS

The bainite found in low carbon steels is a complex structure which changes with austenite processing. The microstructure is comprised of a mixture of a bainitic ferrite matrix and high carbon martensite islands (MA). Both of the constituents can vary with changes in processing.

The bainitic ferrite is equiaxed at slower cooling rates or higher transformation temperatures, but changes to lath-like as the cooling rate increases. Furthermore, the MA becomes smaller with increased cooling rate. The morphology of the MA appears to follow that of the bainitic ferrite.

The kinetics of bainite formation are fairly rapid, mainly because the amount of carbon to be partitioned is low and the autocatalytic factor is large. During continuous bainite transformation in low carbon steel, it can be observed that nearly all austenite transform into bainite. The morphology of low carbon bainite is related to the nucleation rate. Nucleation rate is dependent on the driving force, which is mostly related to two factors: the transformation temperature and the cooling rate. At high transformation temperature, or a slow cooling rate, the nucleation rate of bainitic ferrite is low. Large bainitic sizes are observed, and very similar orientations of bainitic ferrite grains are observed in some austenite grains. Smaller crystal rotations occur when atoms undergo small shear movement during the bainite transformation at a slow cooling rate or during coarsening, results in large and possibly massive bainitic ferrite. The rapid cooling rate gives additional driving force to produce more random orientations of bainitic ferrite and leads to the small bainite size.

Due to the rapid speed of the bainite transformation in low carbon steel, it is more important to control the bainitic ferrite nucleation rate than the growth rate of bainitic ferrite. As analyzed by thermodynamics and kinetics, reducing the bainite nucleation activation energy barrier, such as by (i) increasing the undercooling by increasing the cooling rate or (ii) increasing the stored energy by deformation of the austenite, can increase the nucleation rate, thus refining both the bainitic ferrite size and the accompanying MA.

ACKNOWLEDGMENTS

The authors would like to thank the United Metallurgical Company (OMK), Vyksa, Russia, for its partial financial support of this work, and the United States Steel Research and Technology Center and the Baosteel Research Institute, especially Dr. Sihai Jiao, for in-kind support. In addition, the authors would like to thank BAMPRI and the Materials Characterization Lab in the MEMS Department at the University of Pittsburgh for providing the facilities used to conduct this research.

REFERENCES

1. C. Isaac Garcia, M.J. Hua, X. Liang, P. Suikannen, and A.J. DeArdo: *Materials Science Forum*, Trans Tech, Stafa-Zurich, 2012, pp. 17–23.
2. A.J. DeArdo: *Proc. Int. Conference Microalloying*. 1995. pp 15–33.
3. F.G. Caballero and J. Santofimia: *Novel High Strength, High Toughness Carbide-Free Bainitic Steels: Final Report*, Office for Official Publications of the European Communities, 2007.
4. X. Liang: Ph.D. Thesis, Mechanical Engineering and Materials Science, University of Pittsburgh, 2012.
5. K. Zhu, O. Bouaziz, C. Oberbillig, and M. Huang: *Mater. Sci. Eng. A*, 2010, vol. 527, pp. 6614–19.
6. C.Y. Huang, J.R. Yang, and S.C. Wang: *Mater. Trans. Jim.*, 1993, vol. 34, pp. 658–68.
7. Y. Ohmori: *J. Iron Steel Inst. Jpn.*, 1973, vol. 13, pp. 56–62.
8. G. Krauss: *Steels: Processing, Structure, and Performance*, ASM International, Materials Park, OH, 2005.
9. S. Zajac, V. Schwinn, and K.H. Tacke: *Materials Science Forum*, Trans Tech, Stafa-Zurich, 2005, pp. 387–94.
10. B.L. Bramfitt and J.G. Speer: *Metall. Trans. A*, 1990, vol. 21A, pp. 817–29.
11. H.I. Aaronson, W.T. Reynolds, G.J. Shiflet, and G. Spanos: *Metall. Trans. A*, 1990, vol. 21A, pp. 1343–80.
12. P.P. Suikkanen, C. Cayron, A.J. DeArdo, and L.P. Karjalainen: *J. Mater. Sci. Technol.*, 2013, vol. 29, pp. 359–66.
13. P. Cizek, B.P. Wynne, C.H.J. Davies, B.C. Muddle, and P.D. Hodgson: *Metall. Mater. Trans. A*, 2002, vol. 33A, pp. 1331–49.
14. H.K.D.H. Bhadeshia: *Mater. Sci. Eng. A*, 1999, vols. 273–275, pp. 58–66.
15. G.I. Rees and H.K.D.H. Bhadeshia: *Mater. Sci. Technol. Lond.*, 1992, vol. 8, pp. 985–93.
16. G.I. Rees and H.K.D.H. Bhadeshia: *Mater. Sci. Technol. Lond*, 1992, vol. 8, pp. 994–1003.
17. S.M.C. van Bohemen: *Philos. Mag.*, 2013, vol. 93, pp. 388–408.
18. H.K.D.H. Bhadeshia: *Acta Metall. Mater.*, 1981, vol. 29, pp. 1117–30.
19. H.K.D.H. Bhadeshia and J.W. Christian: *Metall. Trans. A*, 1990, vol. 21A, pp. 767–97.
20. J.C. Bokros and E.R. Parker: *Acta Metall. Mater.*, 1963, vol. 11, pp. 1291–1301.
21. J.P. Naylor: *Metall. Trans. A*, 1979, vol. 10A, pp. 861–73.
22. X.J. Liang, M.J. Hua, C. Isaac Garcia, and A.J. DeArdo: *Materials Science Forum*, Trans Tech, Stafa-Zurich, 2013, pp. 38–46.
23. G.T. Park, S.U. Koh, H.G. Jung, and K.Y. Kim: *Corros. Sci.*, 2008, vol. 50, pp. 1865–71.
24. S.U. Koh, H.G. Jung, K.B. Kang, G.T. Park, and K.Y. Kim: *Corrosion*, 2008, vol. 64, pp. 574–85.
25. E.J. Palmiere, C.I. Garcia, and A.J. DeArdo: *Metall. Mater. Trans. A*, 1996, vol. 27A, pp. 951–60.

26. F.G. Caballero, M.K. Miller, S.S. Babu, and C. Garcia-Mateo: *Acta Mater.*, 2007, vol. 55, pp. 381–90.
27. H. Bhadeshia and R. Honeycombe: *Steels: Microstructure and Properties: Microstructure and Properties*, Butterworth-Heinemann, Oxford, 2011.
28. J.W. Christian: *The Theory of Transformations in Metals and Alloys (Part I+II)*, Elsevier, Oxford, 2002.
29. A.T. Davenport, R.E. Miner, and R.A. Kot: *The Hot Deformation of Austenite*, AIME, New York, NY, 1977, vol. 186.
30. K. Tsuzaki, T. Ueda, K. Fujiwara and T. Maki: *Proc. 1st Jpn. Int. SAMPE Symposium and Exhibition*, Society for the Advancement of Materials and Process Eng., Chiba, Japan. 1989. pp 699–704.
31. H.K.D.H. Bhadeshia: University of Cambridge. IOM communications. 2001.
32. D.A. Porter and K.E. Easterling: *Phase Transformations in Metals and Alloys*, CRC Press, Boca Raton, FL, 1992.